



Technical Report No. 35

ASSESSMENT OF FLOOD PEAK SIMULATIONS BY GLOBAL HYDROLOGICAL MODELS



Author names: James Miller, Thomas Kjeldsen, Christel Prudhomme

Date: September 2011



WATCH is an Integrated Project Funded by the European Commission under the Sixth Framework Programme, Global Change and Ecosystems Thematic Priority Area (contract number: 036946). The WACH project started 01/02/2007 and will continue for 4 years.

Title:	Assessment of Flood Peak Simulations by Global Hydrological Models
Authors:	James Miller, Thomas Kjeldsen, Christel Prudhomme
Organisations:	Centre for Ecology and Hydrology
Submission date:	August 2011
Function:	This report is an output from Work Block 4; task 4.1.3., 4.1.4, 4.3.2
Deliverable	WATCH deliverables: D4.1.3b, D4.3.1b

Abstract

With significant changes to flood frequency anticipated as a result of climate change it becomes important to investigate how global hydrological models process climate forcing data. Flood frequency distribution describes the relationship between flood peak magnitude and its return period, indicating the average period of time between exceedance of a certain flood magnitude. The steepness of the distribution (or of the growth curve) is a measure of the variability of the flood peak series. Analysis of variation in extreme rainfall-runoff processes between global hydrological models was undertaken by comparing the variability in extreme rainfall events of certain frequency in WATCH Forcing Data (WFD) with the resulting variability in flood events as predicted across the models GWAVA, JULES, and WaterGap. Analysis of propagation of climate model biases between global hydrological models JULES and WaterGap compared changes in predicted flood frequency growth curve steepness when applying baseline daily climate forcing simulated by the ECHAM5 climate model time series. The impact of climate change on the probabilistic behaviour of floods is assessed by considering the change in growth curve between the control run conditions and the future scenarios as predicted by ECHAM5-A2 driven time series.

Spatial patterns of variation in extreme rainfall-runoff processes differ between models, particularly in regions of extreme climate, highlighting the importance of using more than one hydrological model. Flood statistics derived from simulations from two hydrological models run with the same forcing climate differ significantly, suggesting that the models are sensitive to different climate characteristics, or that they are calibrated with sub-optimal conditions. Simulated control climate might also have some characteristics different than those of historical observations. Climate change simulations indicate some general agreement between models in the emerging spatial pattern of future changes to flood variability across Europe; however, some distinct regional and sub-regional differences in magnitude of change and spatial pattern are evident. The results obtained in this research are promising, and should be extended to include a larger sample of hydrological and climate models, with more detailed investigation of hydrological model structure and validation of modelled values with observed flow series.

Introduction

Climate change is expected to lead to shifts in the global hydrological cycle, resulting in regional changes in runoff quantity and greater variability in seasonal flows (Arnell, 2003). This will potentially lead to significant changes in flood frequencies and magnitude (Lehner et al, 2005), altering regional flood characteristics. Flood frequency entails estimating the annual possibility of exceedance for a given peak flow. Most commonly this is done using a probability distribution fitted to a series of annual flood maxima extracted from continuous series of runoff data. Continuous time series of global runoff have been modelled at a 0.5° gridded resolution by a suite of hydrological models as part of WATCH. Assessing modelled runoff data for future periods against baseline ‘control-run’ conditions allows a comparison to be made between flood frequency curves, indicating whether extreme flood events will potentially become more common. Differences in the growth curves, calculated between hydrological models, provide an indication of the level of uncertainty inherited in predicting the potential level of change in the flood frequency relationships.

This document details the method and results from undertaking an analysis of annual maximum series of peak flow (described by the total runoff) as simulated by the global hydrological models JULES, GWAVA, and WaterGap. These hydrological models were driven with the same daily climate forcing data at 0.5° resolution, the WATCH Forcing Data WFD (Weedon et al., 2010) to provide a benchmark for comparisons with GCM-driven simulations for the later part of the 20th century. JULES and WaterGap were also driven with daily climate forcing simulated by the ECHAM5 climate model time series, bias corrected to better represent the observed climate (Piani et al., 2008; Piani et al., 2010). Comparison of runoff simulations driven by observed and modelled climate will highlight some of the biases introduced by the climate modelling. Here, the focus is on the representation of the flood extremes, and in particular, to the variability of flood peak, as represented by an index of steepness of flood frequency curve, relative to each simulated time series. Comparison of runoff simulations driven by modelled climate for two time periods (one representative of the baseline, one of the future) will show possible changes in the flood regime as simulated by a particular climate-hydrological modelling chain. By undertaking these comparisons for several hydrological models, it is possible to investigate the influence of the hydrological modelling in the propagation of biases and changes from the climate to flood flows, and evaluate whether hydrological modelling uncertainty is large.

Three global hydrological model were considered: JULES, WaterGap and GWAVA (except for climate-driven simulations as not fully available), while only climate simulations from ECHAM5 were analysed.

Methods/Data

Data selection

WFD-driven daily total runoff output from JULES, WaterGap and GWAVA were selected for analysis of how different hydrological models processed observed WFD hydro-meteorological forcing climate. Data covering the period 1961-1990 were selected, and is in the form of time series for each 0.5° grid of the hydrological models land mask.

ECHAM5-driven daily total runoff from JULES and WaterGap were selected for analysis of simulated forcing data from WATCH WB3 (GWAVA does not have any daily simulations available for the future). Two runs were used depending on the period of analysis: ECHAM5-control, based on historical emission scenarios, provided data for the baseline (1965-1994; 30-year period of available data closest to 1961-1990); and ECHAM5-A2, based on the SRES A2 emission scenario (IPCC, 2000), provided data for the 2070-2099 time horizon.

For each 30-year period (baseline WFD, control and future) the annual maximum series (AMS) of peak flow were extracted from the simulated daily time series of total runoff in each 0.5° grid element and based on a water-year from October to September. Similarly, AMS of one-day WFD rainfall were extracted for each period. A generalised extreme value (GEV) distribution was fitted to each AMS, using the method of L-moments (Hosking and Wallis, 1997). Flood frequency distribution describes the relationship between flood peak magnitude and its annual exceedance probability (AEP). The AEP is more commonly expressed as a return period indicating the average period of time between exceedance of a certain flood magnitude). The steepness of the distribution (or of the growth curve) is a measure of the variability of the flood peak series, and hence of the flood regime of the area of interest. The steepness of the growth curves were quantified as the ratio of the 50- or 100-year to the 5-year quantiles, henceforth referred to as growth curve ratios. The same analysis is done on precipitation daily time series, providing precipitation growth curves.

Runoff simulations using 20th century observed climate data - analysis of variation in extreme rainfall-runoff processes between global hydrological models

From the fitted GEV distribution the precipitation and flow quantiles with a 100-year and 5-year return period (P_{100} and P_5 , Q_{100} and Q_5 respectively) were estimated using data for the baseline period 1961-1990. The differences between hydrological models in the rainfall-runoff transformation process of extreme events can then be assessed by considering the growth curve ratio calculated for the precipitation driving data and comparing the flood growth curve ratio calculated for each model, expressed respectively as;

$$\frac{P_{100}}{P_5} \text{ Precip} \quad \text{and} \quad \frac{Q_{100}}{Q_5} \text{ Flow}$$

Runoff simulations using 20th century modelled climate data - analysis of propagation of climate model biases between global hydrological models

The flood ratios were also derived from the GEV distributions based on simulations driven by the control ECHAM5con for the period 1965-1994. The ratio between the 50-year and 5-year event was chosen as a suitable ratio for comparison. For each hydrological model, the difference between this flood ratio relative to WFD and ECHAM5con simulations is a measure of the biases introduced by the ‘climate-hydrology’ model combinations. It is expressed as;

$$Bias = 100x \frac{\frac{Q_{50}}{Q^5}_{con} - \frac{Q_{50}}{Q^5}_{WFD}}{\frac{Q_{50}}{Q^5}_{WFD}}$$

where subscript ‘con’ refers to the ratio based on ECHAM5con-driven series, and subscript ‘WFD’ refers to the flood ratio based on WFD-driven series.

Runoff simulations using 21st century modelled climate data - analysis of changes in extreme flood variability

The impact of climate change on the probabilistic behaviour of extreme floods is assessed by considering the change in 50-year and 5-year flood growth curve ratios between the control run conditions (con) and the future scenarios (fut), and is expressed as the percentage change as;

$$Change = 100x \frac{\frac{Q_{50}}{Q^5}_{fut} - \frac{Q_{50}}{Q^5}_{con}}{\frac{Q_{50}}{Q^5}_{con}}$$

where subscript ‘fut’ refers to the flood ratio based on ECHAM5A2-driven series for the future, and subscript ‘con’ indicates the flood ratio based on the ECHAM5con-driven series.

An increase in the ratio would suggest a move towards steeper growth curves, i.e. more variability between years in extreme flow events, and vice versa for a decrease. The ratio does not indicate how the magnitude of flooding will be affected. Figure 1 illustrates an example of such a change calculated for a grid cell located on the south-east tip of Spain, whereby the ratio between the Q5 and Q50 event magnitude has increased by 23% with climate change (illustrated by the increase in the steepness of the growth curve gradient between these two return period flows). This results primarily from an increase in the Q50 event, with no associated increase in the magnitude of the Q5 event.

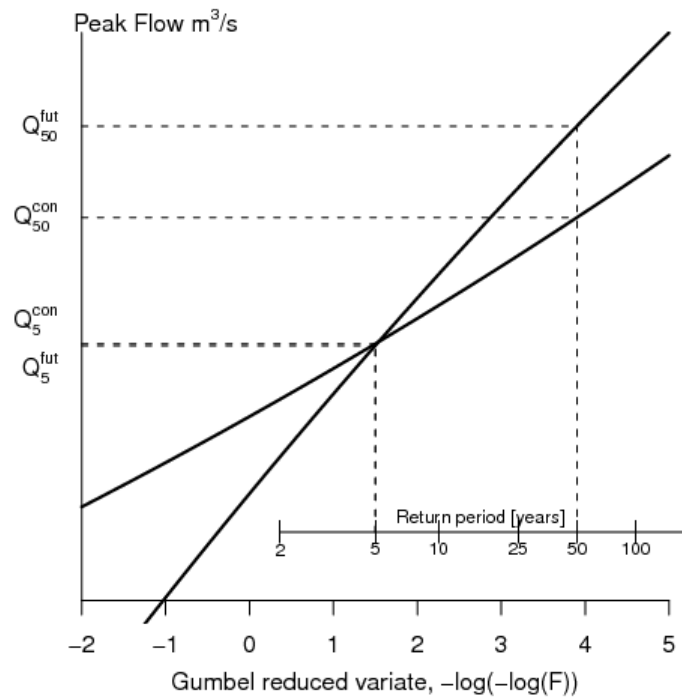


Figure 1: Change in WaterGap flood frequency curve gradient (+23%), resulting from change in quantiles between ECHAM5con-driven series (1965-1994) to ECHAM5-A2 driven series (2070-2099); for grid cell located in SE tip of Spain (Longitude -1.25, Latitude 36.75)

Results

Runoff simulations using 20th century observed climate data - analysis of variation in extreme rainfall-runoff processes between global hydrological models

Global maps of the ratio between the 100-year and 5-year precipitation event derived from the WFD daily precipitation time series (rainfall ratio) and the corresponding flood growth curve ratio, have been calculated from the WFD-driven total runoff daily time series over the period 1961-1990, Figure 2 splits the global land mass into distinct regional zones based on geographic and climatic areas to aid discussion of the global mapping. Precipitation ratios are expected to follow the spatial pattern of mean annual precipitation across the globe, as illustrated in Figure 3. Results are presented for all three global hydrological models using a standardised symbology shown in the accompanying map legend (Figure 4 for precipitation ratio; Figure 4 for flood ratio).



Figure 2: Global map by region (courtesy of www.climate-zone.com)

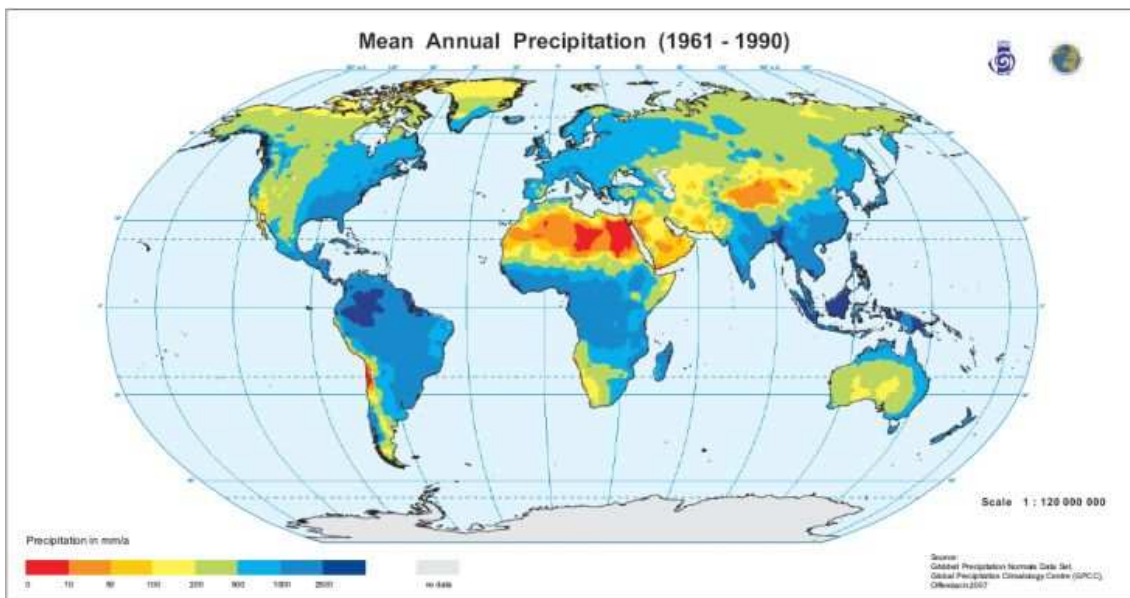


Figure 3: Mean Annual Precipitation (1961-1990). Source: GPCC

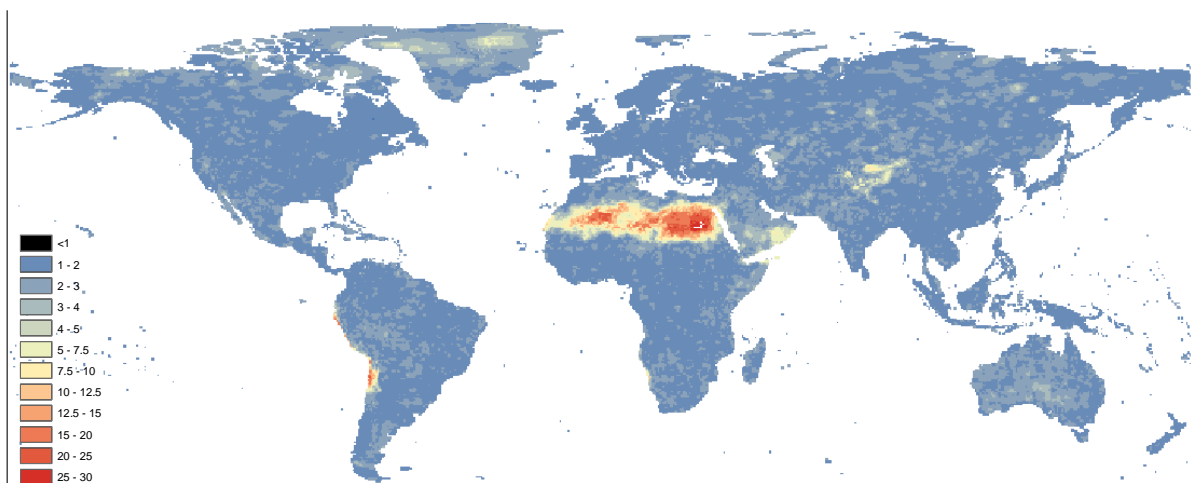


Figure 4: Global mapping of WFD (1961-1990) precipitation growth curve ratio (P100/P5)

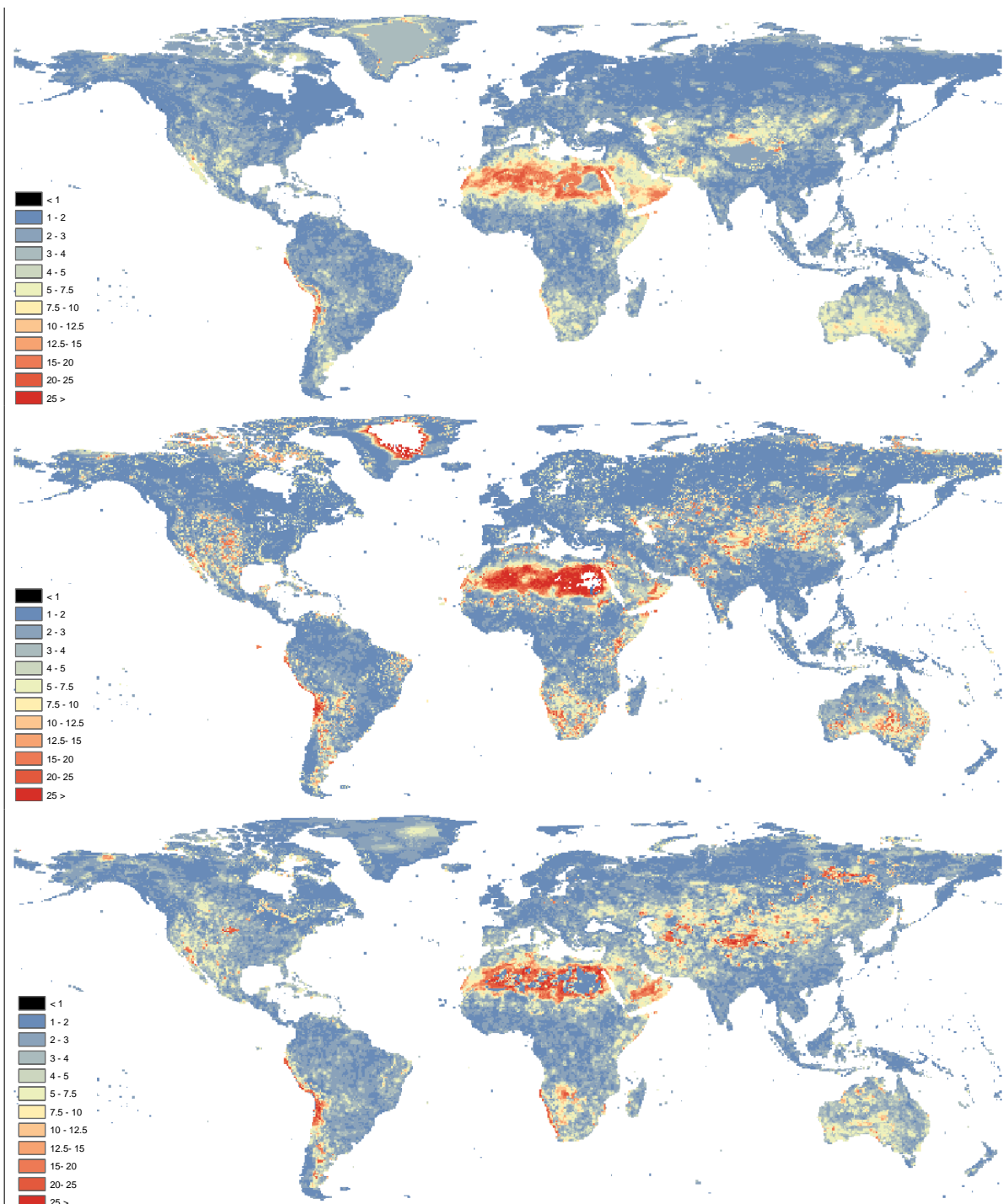


Figure 5: Global mapping of WFD-driven flood growth curve ratio (Q100/Q5) (1961-1990) derived from simulations by GWAVA (top), WaterGap (middle) and JULES (bottom).

North America (including Greenland)

Extreme precipitation ratios are low across most of the entire continent, typically varying between values 1-3. To the very north this rises in some areas up to 5, and even up to 7.5 over certain areas of Greenland.

Across the North American land mass the flood ratio spatial pattern derived from the different hydrological models is similar in places with generally higher flood ratios in the south-

western areas of the USA and northern Alaska. In the rest of the continent, however, there are marked differences between models. JULES is associated with very high values in northern USA, along with an arc of high values in south-east Canada that is not evident in results from the two other hydrological models. WaterGap also shows some similarly high ratios in central and southern USA, but over larger areas than JULES; the spatial pattern of the high flood ratio is also more speckled in nature, showing a lack of spatial smoothness in the simulated extreme flood. High flood ratios are also simulated by WaterGap in northern areas of Canada, particularly in islands to the north.

For Greenland, flood ratios derived from all models differ greatly, with WaterGap showing no data for central areas, and rapidly predicting very high values that diminish towards the coast. For GWAVA, there is a homogenous area covering most of Greenland, with some similar rapid changes from high to low flood ratios towards the coast. JULES simulates a range of low flood ratios with no particular spatial pattern. The difference in the flood ratio derived from the different models on Greenland is likely to highlight the difference in the representation of the snow/rainfall partitioning and snow-melting processes, as Greenland is a land-mass covered in ice during most of the year. Differences in the snow processes was also noted as a main difference in global hydrological models (including GWAVA, JULES and WaterGap) of the Water Model Inter-comparison Experiment by (Haddeland et al., in press).

South America

Extreme precipitation ratios are low across most of the entire continent, varying between values 1-4. However there are very high values up to and even exceeding 20 observed along the Western coast, in a long strip that follows much of the Andes mountain chain and represents the area covered by the Atacama Desert and surrounding areas – one of the driest places on Earth. This is a result from the orographic enhancement of precipitation on the windward zones of the Andes, with long periods of no rainfall interrupted by a few rainfall events – resulting in a very steep precipitation growth curve.

There is broad agreement in the flood ratios as simulated by all models, with very high flood ratios located on the western coast, covering the region of the Andes mountain range. The flood ratio is much higher and covers a greater area for both JULES and WaterGap. Both models also show higher flood ratios compared to GWAVA for far eastern parts of Brazil and north Venezuela. WaterGap flood ratios again seem more speckled in spatial distribution.

Africa

Extreme precipitation ratios are low across most of the continent south and north of the Saharan region, being between 1-4, except for some higher values (5-12.5) in the very south-west and around the Horn of Africa – both very dry regions. In the Saharan region, values vary between 4 and 12.5 on the fringes, and reach over 25 in the most central areas. These precipitation ratios highlight the very high variability in precipitation in this continent, especially in the driest areas. Note the absence of precipitation ratio for seven cells in the eastern Saharan region, for which no precipitation occurred over the period assessed.

Some broad geographic patterns of the flood ratios are shared by all three hydrological models, following the climatic/biome regions of Desert, Rainforest and Savannah regions of the continent. However the detailed spatial patterns within such regions can greatly differ between models.

In Saharan Africa, flood ratios can be extremely high, exceeding 25 in all models – perhaps suggesting unrealistic results in the simulated total runoff the flood ratios have been derived from. Similar conclusion in the realism of the flood ratios could be made for some of the low flood ratios simulated in central Egypt by JULES and GWAVA, for example, likely to result from cells where runoff continue to decrease from a non-nil initialisation as precipitation input remain nil throughout the period; errors/missing data/ no runoff were associated with those grid cells by WaterGap (in black in Figure 4). High flood ratios reflect a region with significant variation in Q5 and Q100 events, expected in arid region with extremely rare precipitation events

Central Africa has low flood ratios across most of the areas of extensive rainforest; however, WaterGap shows a band of high flood ratios to the north not simulated by JULES and GWAVA. To the east there are higher flood ratios located in the horn of Africa according to all models, but spatial patterns along the coast vary.

The region to the south of Africa shows some high flood ratios along the western coast in all models, but this area is much greater and covers some inland areas in JULES, while in WaterGap the speckled spatial patterns of high flood ratios covers the whole area.

Europe

Extreme precipitation ratios are low across most of the entire continent, varying between values 1-4.

Flood ratio values are generally low across most of Europe, rising towards the Mediterranean. However WaterGap indicates much more homogeneous areas of low flood ratios and some isolated grids with higher values, along with some areas of higher flood ratios in north Eastern Europe, mainly Scandinavia. Similarly, JULES shows some isolated grid cells with high flood ratios in the vicinity of Poland that are not seen in other models.

Middle East

Extreme precipitation ratios vary considerably across the Middle East, with values between 1 and 12.5.

Flood ratio values vary considerably between models across the region, in both magnitude and spatial distribution. JULES simulates a swathe of high values to the south-east, and pockets of similarly high values in the north and north-west; while the rest of the region has a patchy spatial distribution of values. The spatial pattern of flood ratio simulated by GWAVA resembles the precipitation ratio spatial patterns, with high values in the south-east and northern areas. Like GWAVA, WaterGap simulates Flood ratios broadly resembling the precipitation ratio pattern, but with much more patchiness in the data, with many isolated cells having values in excess of 20.

Asia

The pattern of extreme precipitation ratios across Asia is patchy, generally varying between 1 and 5. The only exception is the region roughly representing the northern high plains of Tibet, where there is an area of values between 5 and 10.

There are some clear general patterns of flood ratio across the Asian continent for all three hydrological models, with rough agreement on those areas of highest ratios. However these spatial patterns are always quite different from the precipitation ratio spatial patterns. JULES

simulates high flood ratios across large parts of the central Asian landmass, with an area of high values also located in south-central Russia. GWAVA has much lower values than JULES and WaterGap across the whole continent, and has flood ratios patterns closest to the precipitation ratios patterns. There is a large area north of India, roughly where the Tibetan Plateau lies, where flood ratios derived from GWAVA are around 2-3 and differ greatly from those from the other two hydrological models. WaterGap output shows flood ratio with a very patchy spatial pattern, with many more isolated high value grid cells than other models, often in places with no associated high precipitation ratio values. WaterGap also shows high flood ratios across India and South-East Asia, along with northern Russia.

Australia (including Oceania)

Extreme precipitation ratios are low across the entire region, varying between values 1-4.

Flood growth curve ratios for all models do not resemble precipitation ratios in magnitude or spatial patterns. Both JULES and GWAVA simulate flood ratios generally of the same magnitude across the Australian land mass, but with some spatial differences. GWAVA shows large central areas with flood ratios between 5 and 7.5, and some isolated areas with values reaching 12.5; JULES however, simulates some lower or higher values across the same areas; in addition, high flood ratios reaching 15 are simulated over some of northern Australia. WaterGap has yet a different pattern, with flood ratios exceeding 20 across large parts of the continent, and some high values to the east. These results highlight probably some difference in the soil moisture storage capacity of the models, in one of the driest areas of the world.

Relationship between precipitation and flood growth curve ratios

The relationship between the driving precipitation data and the resulting extreme runoff is explored further in Figure 6 and 7, whereby the ratio between the extreme precipitation events is considered against the ratio between the flood events of the same statistical return period.

Figure 6 presents the scatter plots between precipitation and flood ratios for all cells of the global land mask associated with the three hydrological models. For a completely impermeable surface without losses through vegetation, both ratios would be identical (total runoff time series over the cell would be the same as the total precipitation time series), and showed in the graph along the one-to-one line. Through the various hydrological processes (including delays due to storage in the land and vegetation, and water losses through evaporation and transpiration), the rainfall time series will be transformed into runoff time series. The greater the transformation, the more different precipitation and flood growth curve ratios are expected to be. The scattering represents the different ways the hydrological processes included in the hydrological models undertake these transformations.

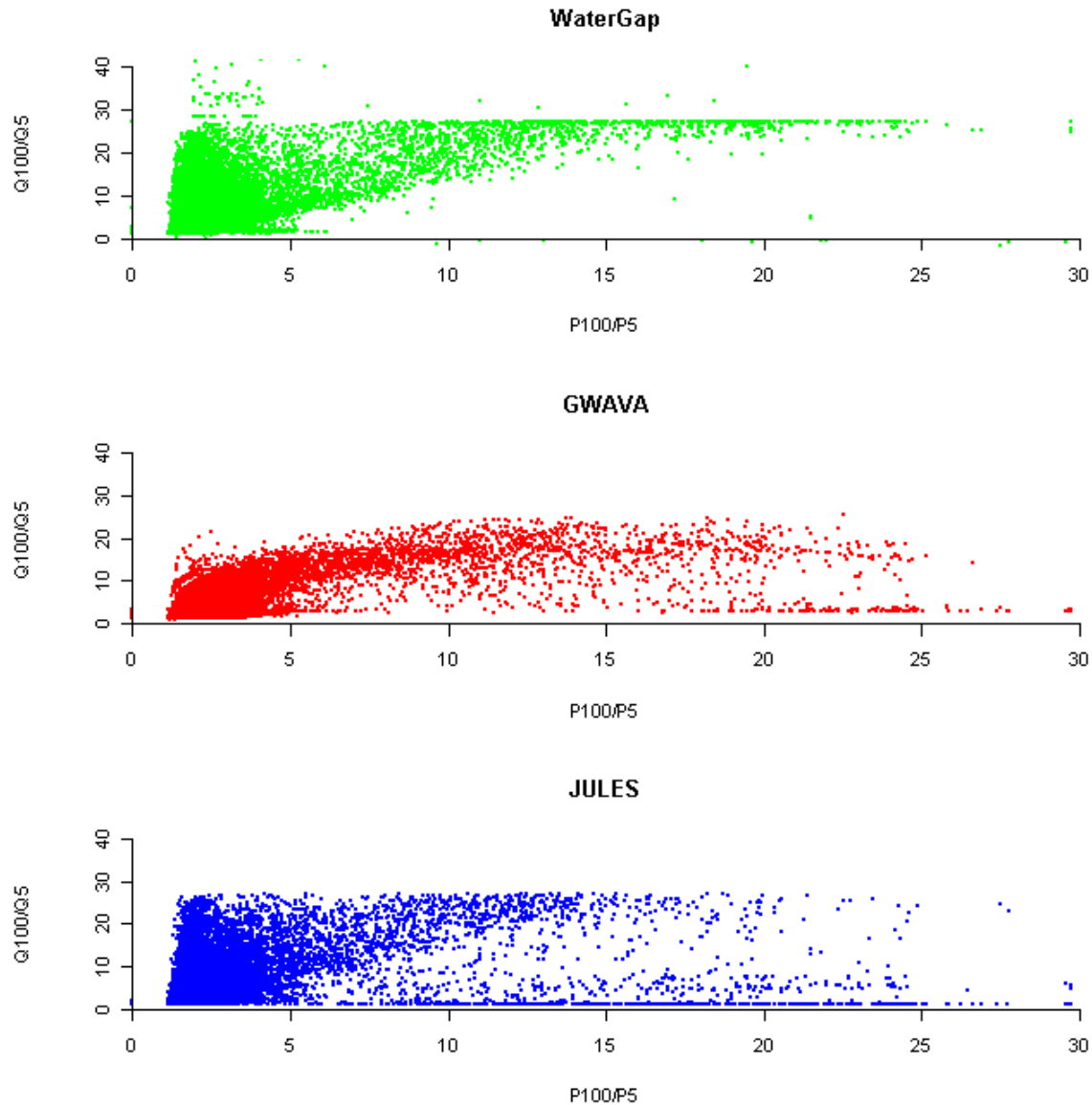


Figure 6: Scatter-plot of precipitation growth curve ratio (P100/P5) against flood growth curve ratio (Q100/Q5) for all models

For greater extreme precipitation variability (i.e. precipitation ratio) influence of the hydrological models start to diverge and those grid cells with precipitation ratios less than 5 are plotted in Figure 7, illustrating how the patterns differ within areas of generally less extreme climate. All grid cells with a precipitation ratio greater than 5 lie within areas of extreme climate, and are limited to the geographical areas including central-western South America (an area composed of the Atacama Desert and surrounding arid areas), the Sahara, Horn of Africa/Middle East, Tibetan Plateau, and Greenland – reflecting the pattern seen in Figure 4. Those areas where the precipitation ratios are highest reflect the spatial pattern of lowest mean annual precipitation observed in Figure 3.

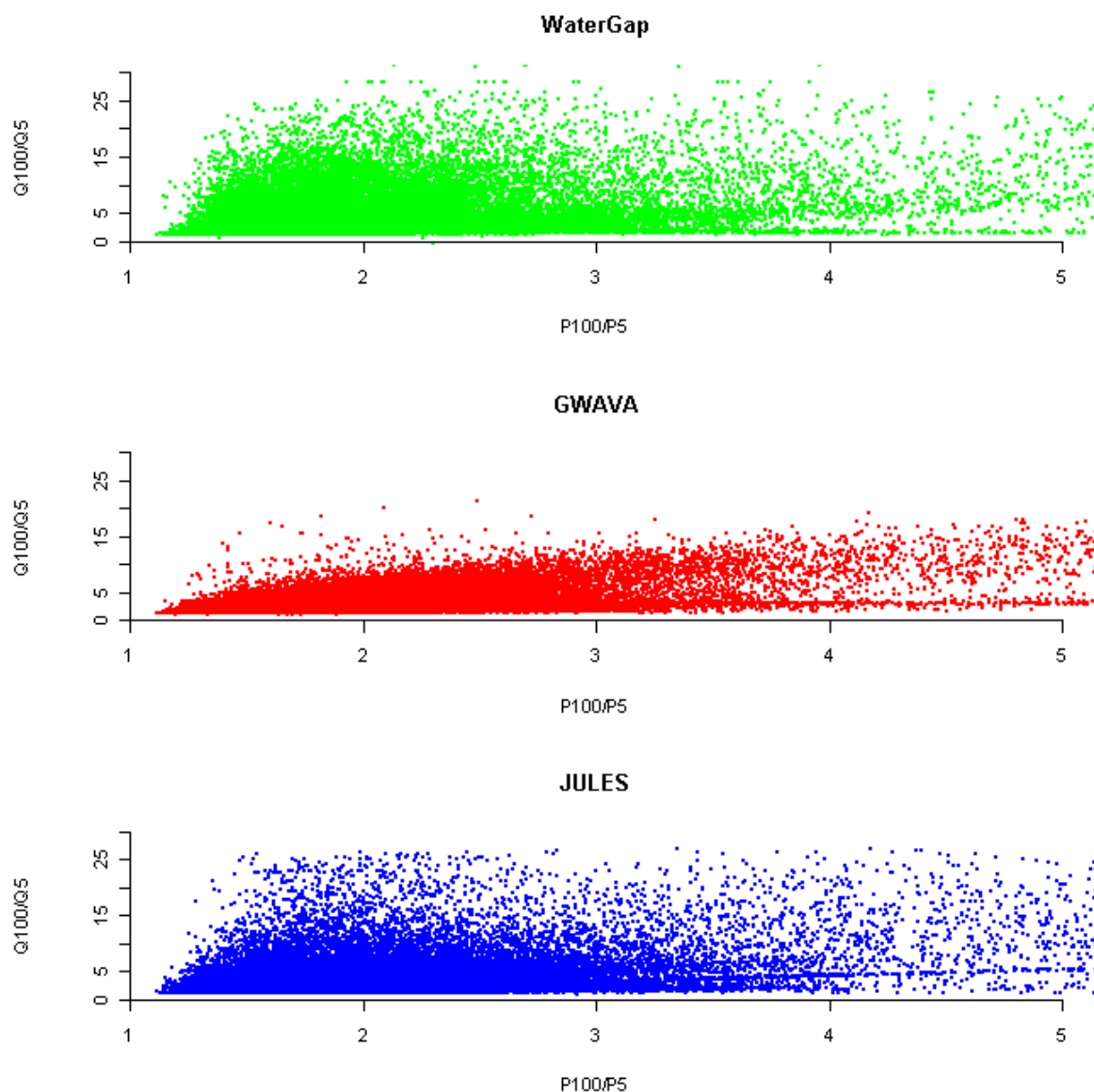


Figure 7: Scatter-plot of precipitation growth curve ratio (P100/P5) against flood growth curve ratio (Q100/Q5) for all models

WaterGap – Some flood ratio (Q100/Q5) are negative, indicating errors in either the simulated runoff time series or in errors during the processing of extremely low runoff values. There are also isolated flood ratios with very high in magnitude, exceeding 30 for grid cells while accompanying precipitation growth curve ratios are lower than 5 – a somehow unrealistic relationship. Finally, there is seemingly a ceiling in the flood ratio around 27, associated with precipitation ratios ranging from 5 to 25, unlikely to represent real physical mechanisms. This could result from the hydrological model parameterisation and initial conditions, with all Q100/Q5 values exceeding 26 occurring exclusively in either the arid Sahara and central-western South America, or the frozen expanses of Greenland.

GWAVA – The scatter-plot between precipitation and flood ratios shows a generally quite plausible pattern, with an increase in the Q100/Q5 associated with increases of P100/P5 ratio when P100/P5 ratio is lower or equal to 15, and with much less scatter below 5 compared to the other models. Note that for some isolated cells, high precipitation ratios are associated

with low flood ratios, suggesting areas where despite a high variability in extreme rainfall events there is little variability between flood events over the same period. These cells, where the precipitation ratio exceeds the value 20, are exclusively located within the arid Sahara and central-western South America regions.

JULES – The scatter-plot between precipitation and flood ratios is generally quite similar to the pattern observed in the WaterGap data, with a high degree of scatter in flood ratios for precipitation ratios below 5. However, there is a lower limit to the Q100/Q5 ratio, associated with a whole range of cells with variable precipitation ratios which might indicate some unrealistic simulated runoff time series. All such grid cells are located exclusively within the arid Sahara and central-western South America regions. There also seem to have an upper limit to the flood ratio, but much less marked than for WaterGap.

Runoff simulations using 20th and 21st century modelled climate data - analysis of propagation of climate model biases between global hydrological models, and analysis of changes in extreme flood variability

Flood statistics derived from the hydrological models JULES and WaterGap driven by the ECHAM5 were analysed for the baseline period 1965-1994 (using the ECHAM5 control run climate as input) and future period 2070-2099 (using the ECHAM5-A2 climate as input). From each resulting daily total runoff time series, the 50-year and 5-year flood quantiles were calculated and corresponding flood ratios derived, providing an index of the steepness of the associated flood growth curve. Two comparisons were made:

- Biases due to the climate/hydrological model combination, as expressed by the percentage difference in the control and WFD flood ratios.
- Changes in the flood ratio between baseline and future time periods, as simulated by a climate/hydrological model combination.

Maps of flood ratios, biases and changes are presented for JULES and WaterGap for Europe and patterns discussed in this section. A standardised symbology has been used for all maps for easier comparison. A zero flood ratio denotes grid cells with no runoff produced.

Maximum flood ratios simulated by WaterGap are significantly greater than the maxima simulated by JULES. While high flood ratios could reflect the impact of changed climate on extreme flood events, those highest ratios are located in few isolated cells, and arguably unrealistic. They might reflect some of the difficulties global hydrological models have in simulating runoff, and could be associated with errors in the simulations rather than showing a real physical feature due to climate change. Changes in the flood ratios can be extreme large, and have been limited to 500% for presentation purposes.

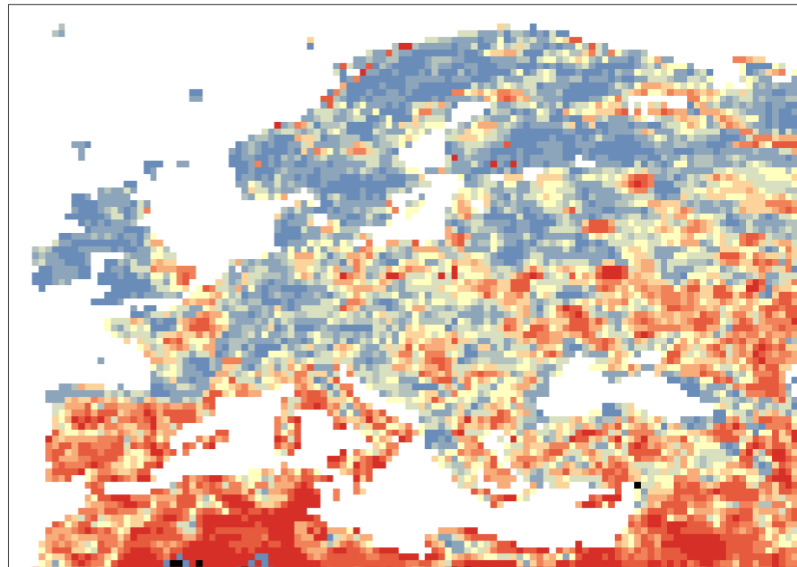
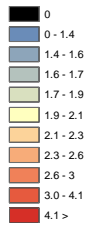
JULES

Figure 8 shows the flood growth curve ratio derived from total runoff time series simulated by JULES driven by (top) WFD climate and (middle) ECHAM5con climate. The differences in the maps should represent the bias introduced by the modelled climate compared to the reference based on WFD. If biases in the climate model were small, both maps should be quite similar – this is somehow expected as a bias correction procedure had been applied to the climate model outputs before input into the global hydrological model (here JULES), aimed to remove most of the systematic biases in monthly climate. This is not the case, with flood ratios derived from ECHAM5con/JULES simulations being much higher than those derived from WFD/JULES simulations in most of Europe. Biases, as expressed by the difference between ECHAM5con- and WFD-driven ratios relative to the WFD-driven ratio, show an overestimation of the flood ratio greater than 100% in all regions except south-west Europe.

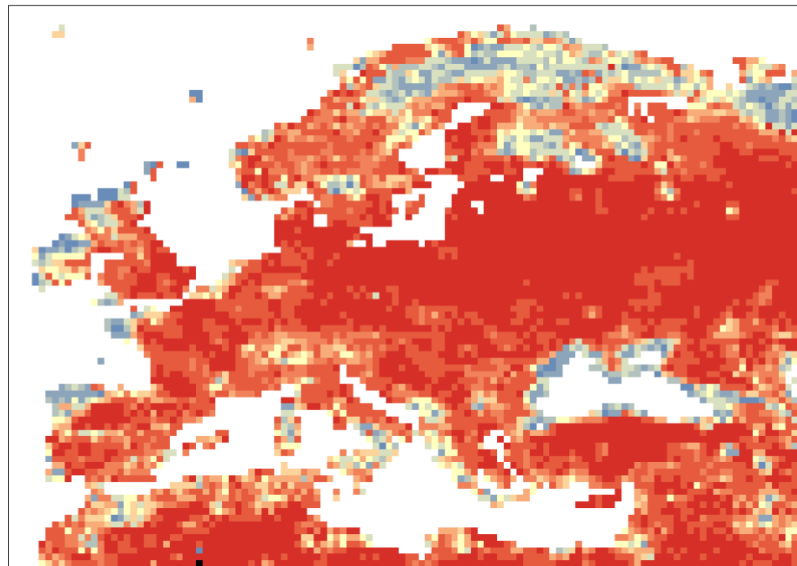
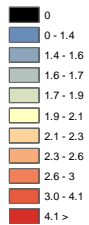
Because the greatest climate factor of influencing extreme flood events is precipitation, as evaporative losses are usually much smaller, it is likely that the differences seen in the flood ratios are mainly due to differences in the ECHAM5con simulated precipitation. This suggests that the bias-correction procedure, which was designed so that the monthly statistics of modelled climate match those of the WFD, is powerless if the climate model fails to simulate realistic temporal rainfall sequencing. This could in turn significantly impact on the way the hydrological model stores water within its sub-surface and groundwater stores, as stores can only replenish when they are not saturated, which is dictated partly by the size of the stores and by the sequencing and intensity of rainfall.

It is out of scope of this paper to investigate further the possible reasons of such discrepancies. This will be done in future collaboration with climate and hydrological modellers.

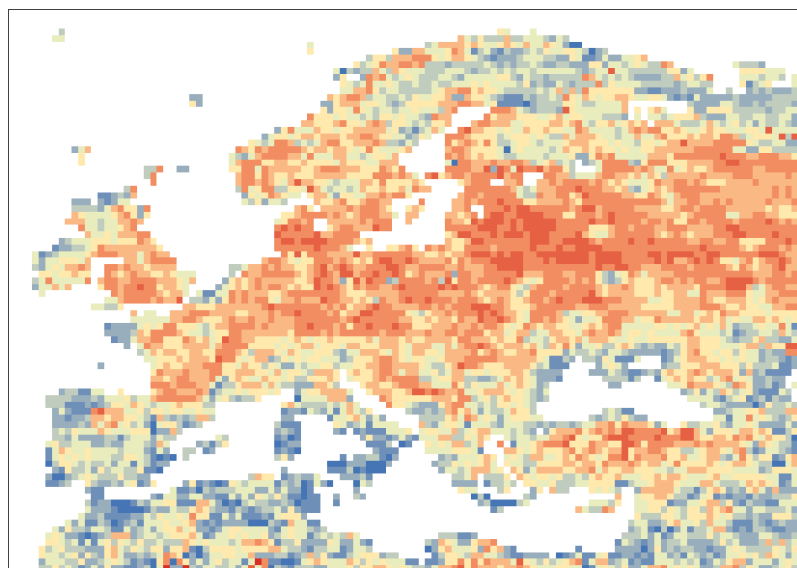
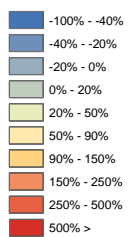
Figure 9 shows flood ratios derived from runoff simulations from JULES using ECHAM5 climate as input for a baseline (top) and future (middle) time horizon. The differences (bottom) express the changes projected to occur by this climate/hydrological model combination. Except for North Africa, the Mediterranean coast, Atlantic coastal areas, and the north Scandinavian coast, flood growth curve ratios are generally projected to decrease by over 20% between the 1970s and the 2080s. This would suggest a reduction of the variability in the flood extremes, either due to an increase in the magnitude of small, common flood events compared to that of rarer floods; or a decrease in the magnitude of the largest flood events; or a combination of the two. These results, however, should be treated with caution as significant biases in the simulation of flood ratios by ECHAM5/JULES modelling chain have been identified.



JULES with
WFD
1965-1995

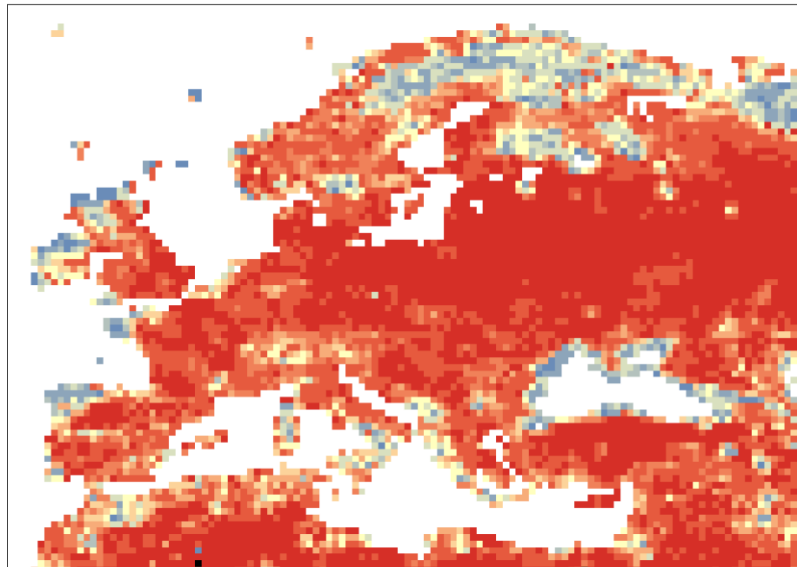
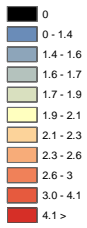


JULES with
ECHAM5con
1965-1994

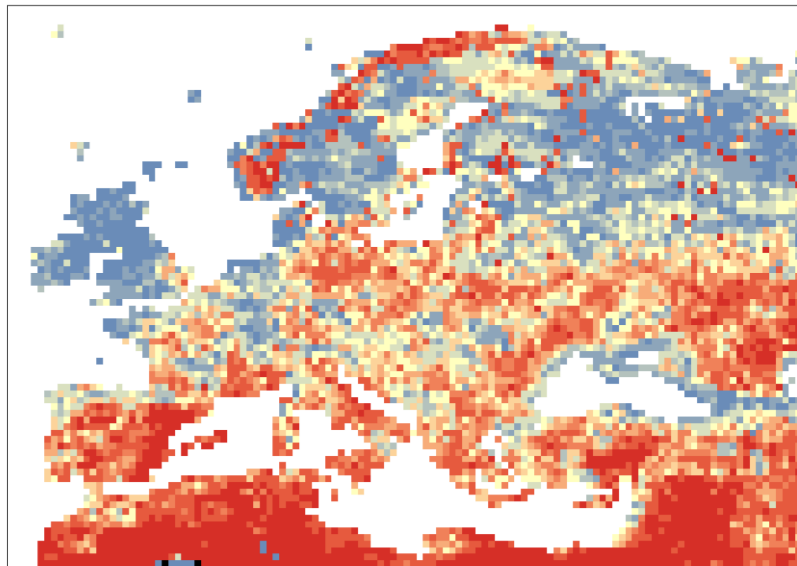
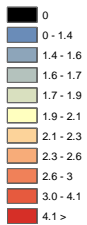


Bias (%
difference)
between
WFD-JULES
and
ECHAM5con-
JULES
1965-1994

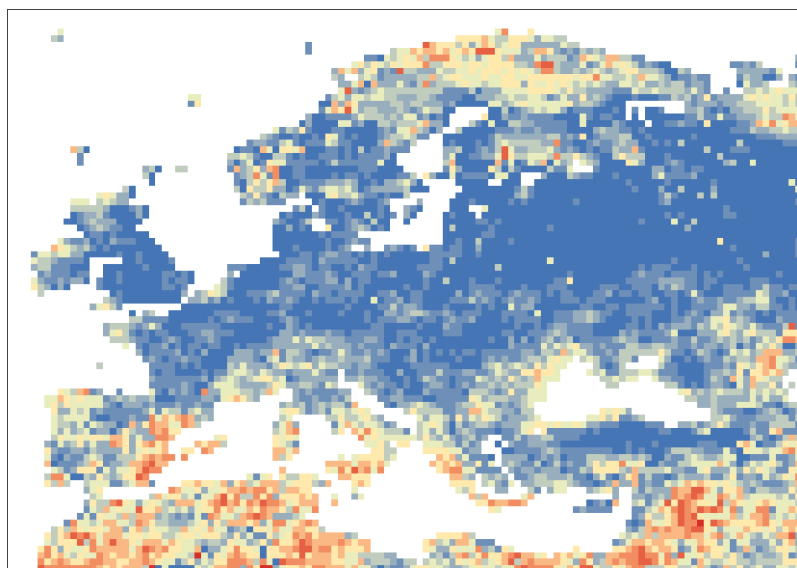
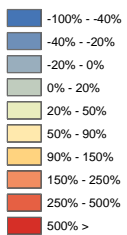
Figure 8: JULES – growth curve ratio (1965-1994) as simulated with: WFD climate (top); ECHAM5 control climate (middle); and bias in growth curve ratio (difference between ECHAM5 and WFD (1965-1994))



JULES with
ECHAM5con
1965-1994



JULES with
ECHAM5A2
2070-2099



Changes (%
difference)
between
ECHAM5con
-JULES and
ECHAM5fut-
JULES
(1965-1994 vs
2070-2099)

Figure 9: JULES - growth curve ratio simulated with ECHAM5/A2 climate for: baseline period (1965-1994) (top); future period (2070-2099) (middle); and change in growth curve ratio (difference between future and baseline) (bottom).

WaterGap

Figure 10 presents the flood growth curve ratios derived from WaterGap total runoff simulations driven by WFD (top) and ECHAM5con (middle) for the 30-year period 1965-1994. For easier comparison, the percentage differences in the flood ratios between the two runs relative to the WFD-driven simulation are also mapped (bottom).

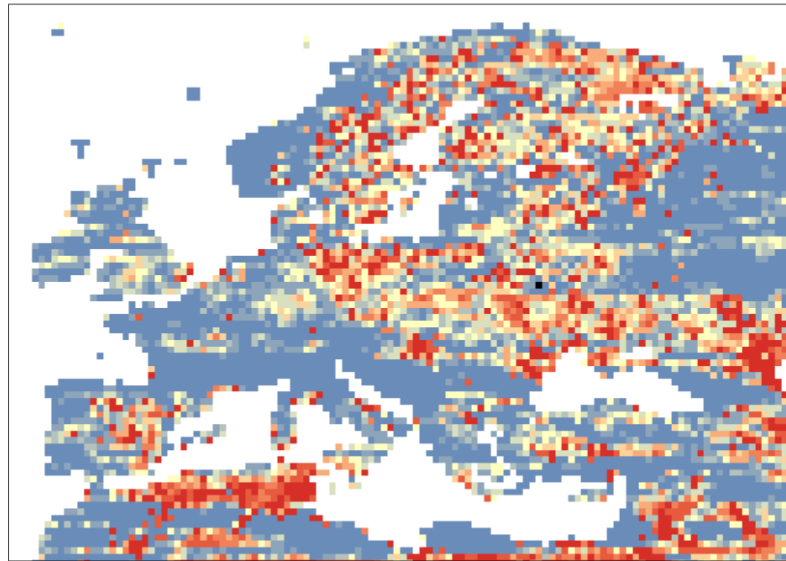
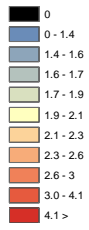
The flood ratio of both WFD and ECHAM5con simulation show a relatively similar spatial pattern, with North Africa, eastern Spain, Sweden and central Europe characterised by flood ratios greater than 1, while there are lower than one for the rest of the continent. However, there is a very large grid-to-grid variation in the flood ratio, with cells showing flood ratios greater than 4 surrounded by cells with a flood ratio lower than one; this patchiness is found for both simulations, and is more likely to result from the model parameterisation than from the climate input data, as the climate signal (as seen in Figure 4 does not have such a pixel-like spatial pattern).

When biases introduced by the ECHAM5 input are quantified, they show an east-west band covering southern France, northern Italy right through the Caucasus with biases over +20%, while they are generally negative in surrounding areas. Overestimations are also located in the inland areas of North Africa, and towards Russia, but remain generally lower than 50%. Patchiness remains in the spatial pattern of biases, confirming a possible origin from the hydrological model rather than the climate model.

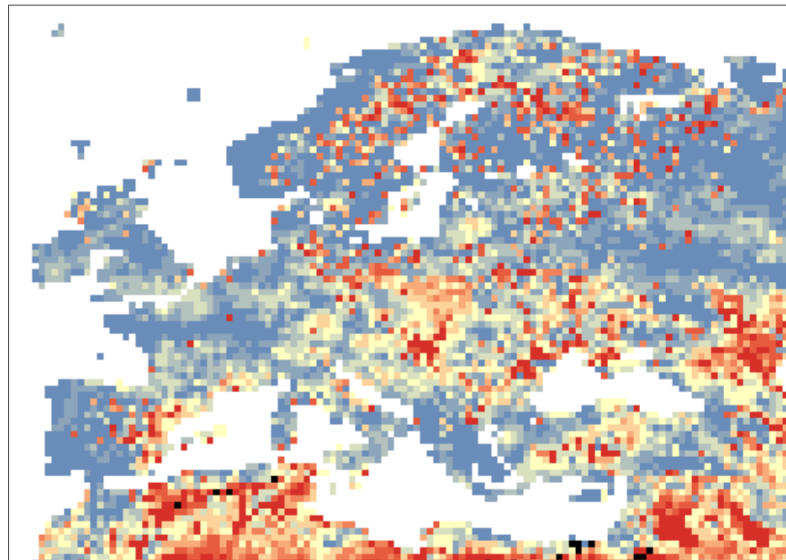
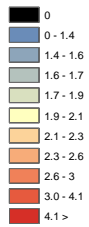
Figure 11 shows simulations from ECHAM5/WaterGap modelling chain for the baseline time horizon (top) and the 2080s future time horizon (middle). Percentage changes between the two are given in the bottom frame.

There is a strong signal of increase in the flood ratio in most of the Iberian peninsula except western and northern coasts, with an increase in the floor ratio greater than 90%. North Africa and eastern Mediterranean fringe also show pockets where flood ratio is projected to increase by more than 90%. An arc from Greece to Ukraine shows projected increase in the flood ratio, albeit of between 20 and 90%. In contrast, for most of north and western Europe the flood ratio is projected to decrease, suggesting the difference between extreme and middle size flood events to be reduced. This reduction is most visible in northern Scandinavia where it is projected to decrease by more than 40%.

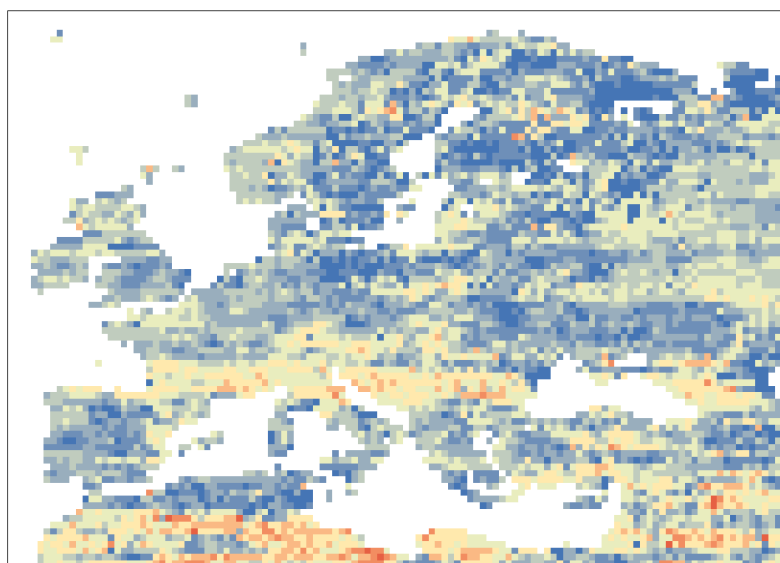
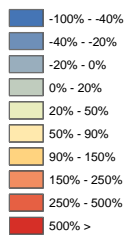
The patchiness in the spatial pattern of the flood growth curve ratio observed for the 20th century simulation remains for the 2080s projections – and to a lesser extent is visible when percentage changes in the flood ratio are calculated. This suggests that there is a need to investigate further the total runoff simulation from WaterGap, and that caution must be taken when interpreting the results.



WaterGap
with WFD
1965-1995

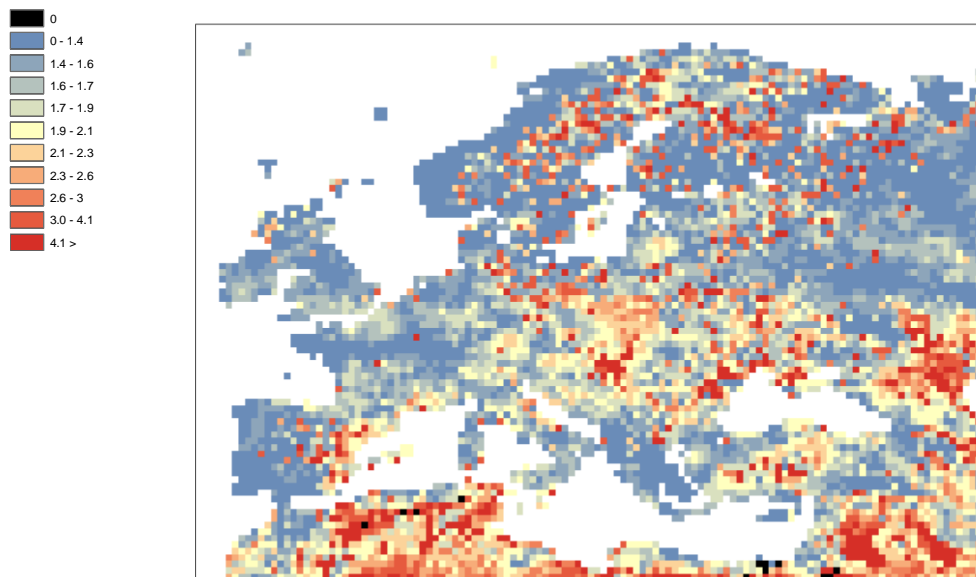


WaterGap
with
ECHAM5con
1965-1995

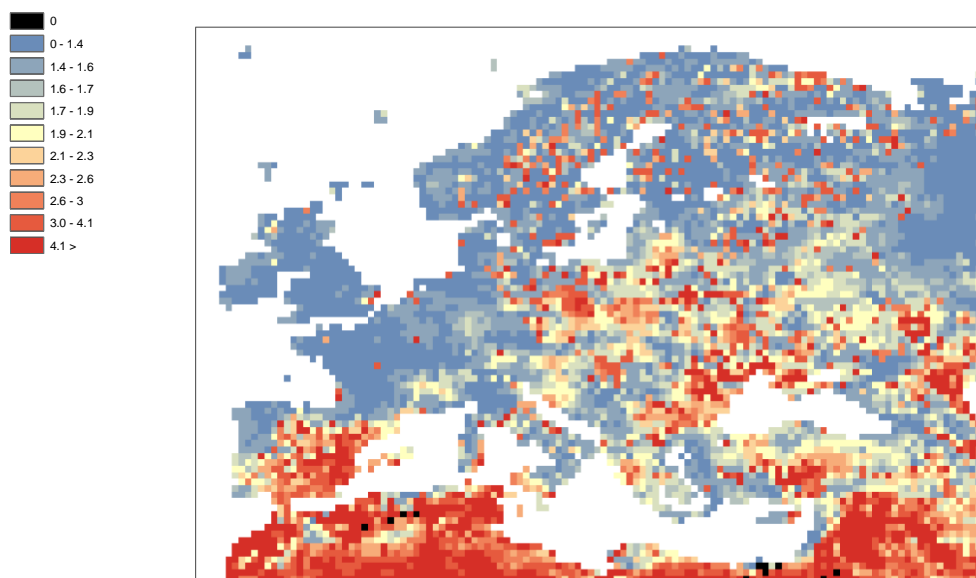


Bias (%
difference)
between
WFD-
WaterGap and
ECHAM5con-
WaterGap
1965-1994

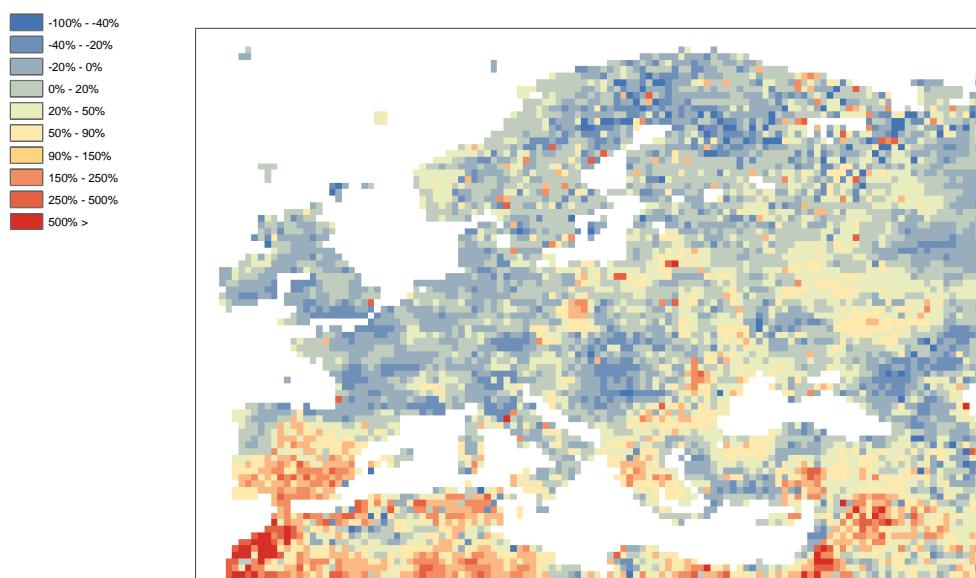
Figure 10: WaterGap - growth curve ratio (1965-1994) as simulated with: WFD climate (top); ECHAM5 control climate (middle); and bias in growth curve ratio (difference between ECHAM5 and WFD) (1965-1994)



WaterGap with
ECHAM5con
1965-1995



WaterGap with
ECHAM5A2
2070-2099



Changes (%
difference)
between
ECHAM5con-
JULES and
ECHAM5fut-
JULES
(1965-1994 vs
2070-2099)

Figure 11: WaterGap - growth curve ratio simulated with ECHAM5/A2 climate for: baseline period (1965-1994) (top); future period (2070-2099) (middle); and change in growth curve ratio (difference between future and baseline) (bottom)

Discussion

Historical data - analysis of variation in rainfall-runoff processes between models

Despite all hydrological models using the same climate forcing data over the late 20th century period 1961-1995, spatial patterns in the flood growth curve ratio simulated by JULES, WaterGap and GWAVA can differ. The differences are greatest in regions of extreme climate, such as northern latitudes and in high-altitude mountain systems, where water is stored as ice and snow for a significant part of the year; or in austral, arid areas such as southern Africa and Australia, where the balance between precipitation input and evaporation losses is extremely variable. This highlights the difficulties for any model to simulate a very large range of hydrological processes, determined not only by the physical characteristics of the land (such as geology and vegetation, for example), but also by the climatic factors. The greatest differences between the precipitation forcing data growth curve ratios and resultant flood growth curve ratios exist in the most extreme areas of climate – encompassing the Sahara Desert, Atacama Desert and surrounding area, Tibetan plateau, south-west Africa (encompassing the Namib Desert), and the ice-fields of Greenland. Despite such differences, however, the overall statistical characteristics of the extreme flood events as simulated by the three models are consistent with those of the extreme precipitation events, suggesting that the saturation processes which result in high runoff are generally all well simulated.

While JULES and GWAVA show relatively similar flood ratios at the world scale, and show a spatial pattern relatively smooth, consistently with expected continuity in physical and climatic properties at the 0.5° scale, while simulations from WaterGap are markedly different. In particular, they are characterised by a speckled pattern of high flood ratios which can be surrounded by grid cells of low flood ratio – this pattern is not confined to a specific region, but can be observed across all continents. When focusing on Europe, this becomes particularly evident. While this is not the scope of this report to investigate in detail what could be the cause of such behaviour, and whether this reflects a real physical phenomenon, it could be argued that some of the internal parameterisation of the model might be the cause, with possibly a discontinuity in some of the store parameters from grid-to-grid. This should be investigated further in collaboration with hydrological modellers.

The analyses undertaken have not sought to provide any quantitative assessment of variability in the magnitude of extreme events simulated by the different hydrological models. However, in assessing differences in the growth curve ratio between the precipitation data driving models and the resulting modelled runoff data, there is a clear indication of differences in the prediction of flood events between models. This highlights the importance of using more than one hydrological model, so that an un-biased and comparative assessment of modelled runoff can be undertaken, but also that perhaps more suitable models should be chosen when consideration of extreme flow events is the focus of analysis. This is particularly important when models are driven with modelled climate data for future periods and changes to the extremes of flow are of interest.

Climate change modelling - analysis of changes in extreme flood variability

The sensitivity of the hydrological models to the driving climate data was tested by comparing the flood growth curve ratios derived from simulations based on the WFD and the ECHAM5con, over the same historical period 1965-1994. Only JULES and WaterGap were considered as no daily simulation was available for GWAVA.

There is a very noticeable difference in the results from JULES, where ECHAM5con-driven simulations generate much greater flood ratios, suggesting much greater variability in the extreme flood peaks than when simulated from observed data. The bias introduced by the ECHAM5con climate is not so marked when simulations are done with WaterGap, but increase in the flood ratio is also noticed in some places. This would suggest that it is possible that the climate simulated by ECHAM5con might have some characteristics different than those of historical observations. As flood events are primarily sensitive to changes in the precipitation regime, this difference is likely to be linked to the day-to-day sequencing of wet/dry episodes, and possibly a higher variability in the precipitation intensity in ECHAM5con than has been observed. Such an inter-monthly bias is difficult to correct with methods such as developed within WATCH by (Piani et al., 2008), in particular due to the very large data requirement for their implementation. The fact that the flood statistics (and in particular the flood ratio) derived from simulations from two hydrological models run with the same forcing climate differ so significantly (as this is the case for ECHAM5con/JULES and ECHAM5con/WaterGap) suggests that the models are sensitive to different climate characteristics. It is not the scope of this paper to investigate in detail the full sensitivity of the global hydrological models, nor the reasons behind the different sensitivity. This might be done by a thorough analysis of some runoff time series for selected grid-cells with contrasting flood ratios, and by collaborations with climate and hydrological modellers.

Changes in the flood ratio were also assessed by comparing results from simulations representative of two time horizons: the historical baseline as represented by the ECHAM5con climate for 1965-1994 and the 2080s future as represented by ECHAM5A2 for 2070-2099. For both hydrological models, there is a suggestion that the variability in the flood extreme could decrease in the future, expressed by a decrease in the flood ratio for most of north and western Europe, and an increase in this variability in southern Spain and north Africa. However, it is also clear that there are some regional differences in the projections from JULES and WaterGap, with a much more marked decrease when simulated by JULES. However, both hydrological models showed some difficulties in reproducing the spatial pattern of historical flood ratio when run with ECHAM5 climate. The results obtained here regarding the possible change in the flood frequency characteristics over Europe must then be considered with caution until more research has been done on the climate-hydrological modelling chain.

Spatial analysis of data

The research reported here aimed to provide a first assessment of some of the differences in the extreme flood characteristics as simulated by different combinations of climate and hydrological modelling tools. It is important to remember that the analysis is focused on extreme events and not long-term flow regimes. It is reassuring that the results show, at the world scale, that the resulting flood characteristics are consistent with the characteristics of the precipitation input – perhaps unsurprisingly as for such extreme events, the complex

hydrological processes generally simplify to a more linear rainfall-runoff transformation, due to the reduction of storage after soils are saturated.

This first broad-brush analysis has, however, highlighted two fundamental results:

- The difference in the way hydrological processes are represented within the global hydrological models impacts on the simulation of the highest flows, and the uncertainty due to the hydrological model is noticeable. It is therefore important to consider more than one hydrological model when undertaking an analysis of extremes. In particular, some hydrological models are much more sensitive to the precipitation temporal pattern than others, as seen with the JULES simulation of the 20th century period;
- Both models JULES and WaterGap have showed some difficulties in representing the flood frequency characteristics – JULES with a very large sensitivity to climate input, WaterGap with an (arguably) unrealistic spatial variability at the sub-regional level that would not be expected.

This suggests that such frequency analysis is a useful tool to evaluate the ability of gridded hydrological models to reproduce the very extreme hydrological events.

Implications for future research

The results obtained in this research are promising, and should be extended to include a larger sample of hydrological and climate models. More specifically, future investigations could include:

- Ascertain physical attributes of the land surface upon which model parameters and variables are based, and explore the relationships between such variables and the patterns observed;
- Explore differences in the AMS between hydrological models, assessing variation in both temporal distribution and magnitude of annual maximum events;
- Calculate and compare quantitative values for flood magnitude at certain return periods between models/periods. Such analyses would also benefit from comparison with values calculated from observed catchment river flow time series, in order to provide an assessment of accuracy in the modelling of extreme events.

References

- Arnell, N. (2003) Effects of IPCC SRES emissions scenarios on river runoff: a global perspective. *Hydrology and Earth System Sciences*, 7(5), 619-641.
- Haddeland I, Clark DB, Transsef W, Ludwig F, Voss F, Arnell NW, Bertrand N, Best M, Folwell S, Gerten D, Gomes S, Gosling SN, Hagemann S, Hanasaki N, Harding R, Heinke J, Kabat P, Koirala S, Oki T, Polcher J, Stacke T, Viterbo P, Weedon GP, Yeh P (in press) Multi-model estimate of global terrestrial water balance: setup and first results. *Journal of Hydrometeorology*, Water and global change special collection.
- Hosking, J. R. M., Wallis, J. R. (1997) *Regional frequency analysis: an approach based on L-moments*. Cambridge University Press, 224 pp.
- Lehner, B., Döll, P., Alcamo, J., Henrichs, J. and Kaspar, F. (2006) Estimating the Impact of Global Change on Flood and Drought Risks in Europe: A Continental, Integrated Analysis, *Climatic Change*, Volume 75, Number 3, 273-299.
- IPCC (2000) *Special report on emissions scenarios (SRES): A special report of Working Group III of the Intergovernmental Panel on Climate Change*. Cambridge University Press, Cambridge.
- Piani C, Haerter JO, Hagemann S, Allen M, Rosier S (2008) *Practical methodologies to correct biases in climate model output, and to quantify and handle resulting uncertainties in estimates of future components of the global water cycle - WATCH Technical report 6*. p. 17.
- Piani C, Weedon GP, Best M, Gomes SM, Viterbo P, Hagemann S, Haerter JO (2010) Statistical bias correction of global simulated daily precipitation and temperature for the application of hydrological models. *Journal of Hydrology* 395:199-215.
- Weedon GP, Gomes S, Viterbo P, Osterle H, Adam JC, Bellouin N, Boucher O, Best M (2010) *The WATCH forcing data 1958-2001: a meteorological forcing dataset for land surface and hydrological models - WATCH Technical report 22*. p. 41.